applied sciences

MDPI

Article

Spatiotemporal Assessment of Air Quality and Heat Island Effect Due to Industrial Activities and Urbanization in Southern Riyadh, Saudi Arabia

Abeer Salman [1,*], Manahil Al-Tayib [2], Sulafa Hag-Elsafi [1], Faisal K. Zaidi [3] and Nada Al-Duwarij [1]

[1] Department of Geography, King Saud University, Riyadh 11564, Saudi Arabia; shagelsafi@ksu.edu.sa (S.H.-E.); nadahamadmohammad@gmail.com (N.A.-D.)
[2] Department of Quantitative Analysis, King Saud University, Riyadh 11564, Saudi Arabia; maltib@ksu.edu.sa
[3] Department of Geology and Geophysics, King Saud University, Riyadh 11564, Saudi Arabia; fzaidi@ksu.edu.sa
* Correspondence: abalsalman@ksu.edu.sa

Abstract: The aim of this paper is to evaluate the air and thermal pollution in the southern suburbs of Riyadh, where people are suffering from poor air quality due to the rapid development of the industrial facilities in the area. The study involved the distribution of questionnaires to 405 residents living in that area in order to obtain their opinions about air pollution. In addition, land surface temperature and 12 components of air were measured at 18 points. In addition, the air quality data from 2016 to 2020 for Al Khaldya and Southern Ring Road air stations were assessed. Al Misfat (Oil Refinery) and the Second Industry City are significant contributors to air pollution and also result in the urban heat island effect from high temperature due to factories and industrial activities. However, all the measured components of air quality are lower than the standard limits except the element particulate matter (PM)10, which exceeds the standard limits in several parts of the study area and during several months of the year. This can surely have a negative impact on the health of residents. At the same time, this study found that the preventive measures taken to stop the spread of COVID-19 infections have led to a positive impact in the area in terms of improvement in air quality.

Keywords: air pollution; Riyadh; industrial city; land surface temperature; geostatistic

Citation: Salman, A.; Al-Tayib, M.; Hag-Elsafi, S.; Zaidi, F.K.; Al-Duwarij, N. Spatiotemporal Assessment of Air Quality and Heat Island Effect Due to Industrial Activities and Urbanization in Southern Riyadh, Saudi Arabia. *Appl. Sci.* **2021**, *11*, 2107. https://doi.org/10.3390/app11052107

Academic Editor: Tung-Ching Su

Received: 8 January 2021
Accepted: 19 February 2021
Published: 27 February 2021

1. Introduction

Urbanization and industrialization are the main sources of air pollution in the world. Consequently, air pollution has become the main topic of many environmental studies [1–5]. The World Health Organization states that air pollution is a threat to human health and is responsible for millions of deaths annually [6–9]. Annually, about 21,000 Canadians die due to exposure to polluted air [10].

Several studies have shown a positive correlation between cancer and exposure to polluted air in different parts of the world [11,12] and in the Arabian Peninsula [13]. The industrial areas in the world are the main contributors to air pollution and are responsible for the deteriorating health of the population.

In Riyadh, the capital of Saudi Arabia, industrialization has increased dramatically during the past couple of decades in response to the increase in population and urban development. Establishment of two industrial cities has resulted in better employment opportunities and, consequently, a high population growth of about 4% in Riyadh [14]. The First Industrial City was established in 1973 and has an area of 0.5 km^2. The Second Industrial City was established in 1976 and has an area of 19 km^2 [15].

Though the Second Industrial City and the Saudi Aramco Oil Refinery (Al-Misfat) were established in the south of Riyadh, far from the city, urban expansion and associated economical activities forced the people to live around the industrial cities. Accordingly,

overcrowded buildings, especially along roads; an increase in traffic and vehicular emissions; and frequent desert dust storms in the area were the principal sources that increased the level of environmental pollutants [16], leading to air pollution [17]. The cumulative effect of these factors resulted in deterioration of air quality indoors and outdoors at many sites in Riyadh [18].

During several visits to the study area in southern Riyadh, it was evident that the area is suffering from multiple aspects of pollution, reduction in visibility during the mornings, and dirty and eroded buildings. Accordingly, residents and workers complained of unhealthy air quality in the area.

Several efforts have been made to study the concentration of chemicals and particulate matter in the air in Saudi Arabi [19–21]; however, most studies were limited and not comprehensive due to insufficient data [18]. As a result, the Royal Commission for Riyadh City and the General Authority of Meteorology and Environment Protection are operating 32 air quality control stations in Riyadh, over the past few years, to monitor the air quality. Some of these monitoring stations are fixed, whereas others are mobile. In addition, the General Authority of Meteorology and Environment Protection launched a dashboard for Riyadh air quality [22] to visualize the air quality index (AQI).

Mapping techniques are useful to assist decision makers in quantifying and locating pollution sites, even with limited measurements. (Geographic information system) GIS and remote sensing are useful tools for spatial analysis and detection of thermal pollution. Geostatistics is a strong technique to assess the spatial analysis of the studied variables [23]. The kriging technique is widely used for investigating sources of pollution as it is a reliable technique with fewer errors, even with small samples [24–26]. In addition, remote sensing imageries, especially in the thermal bands, provide simpler and more accurate information about surface temperature and emissivity [27] to detect urban heat islands (UHIs) [28–30].

Accordingly, this study aims to shed light on the opinions of residents living in southern Riyadh, near the industrial city, regarding emissions of oxides and particulate matter from industrial areas and traffic congestion. Most studies when surveying about the quality of life in cities do not take into account people's opinions about air pollution aspects. The spatial and temporal changes in thermal and air pollution were evaluated from 2016 to 2020. Additionally, the impact of the lockdown on air quality during the coronavirus pandemic was also assessed.

2. Materials and Methods

2.1. Study Area

The study area is located in the southern suburbs of Riyadh. It lies between the coordinates 24.482–24.594 North and 46.759–46.946 East (Figure 1). It covers about 128.7 km^2 and includes the following seven districts: Ad-Difa, Al-Iskan, the second Industrial City, Al-Misfat, Al-Mansuriah, Ad-Dar Al-Baida, and Taybah.

The total number of inhabitants in the study area is 116,510 [31]. The Second Industrial City, including Al Iskan and Ad Dar Al Baida, has a higher population due to better infrastructure and amenities (Figure 2).

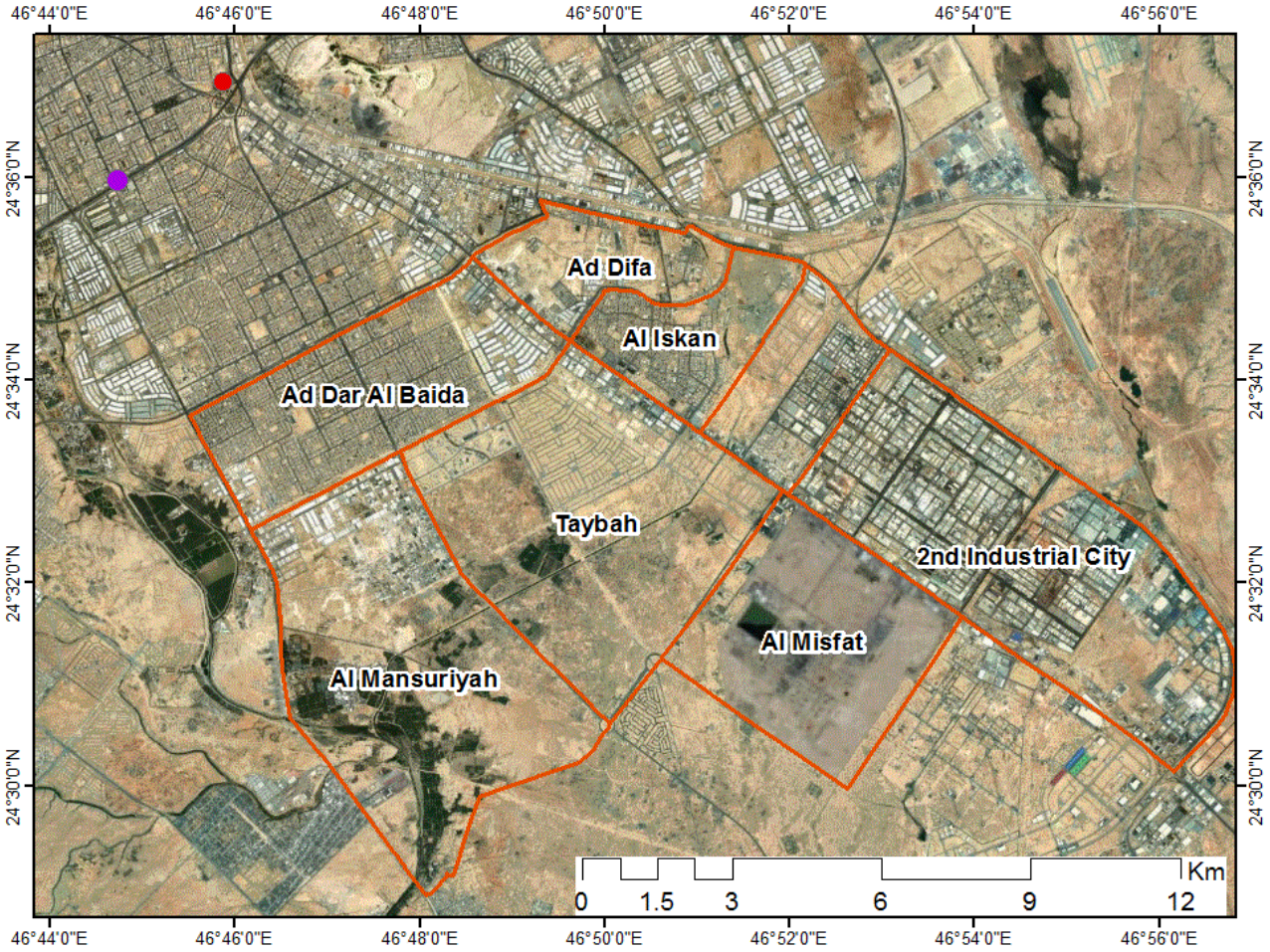

Figure 1. Study area location.

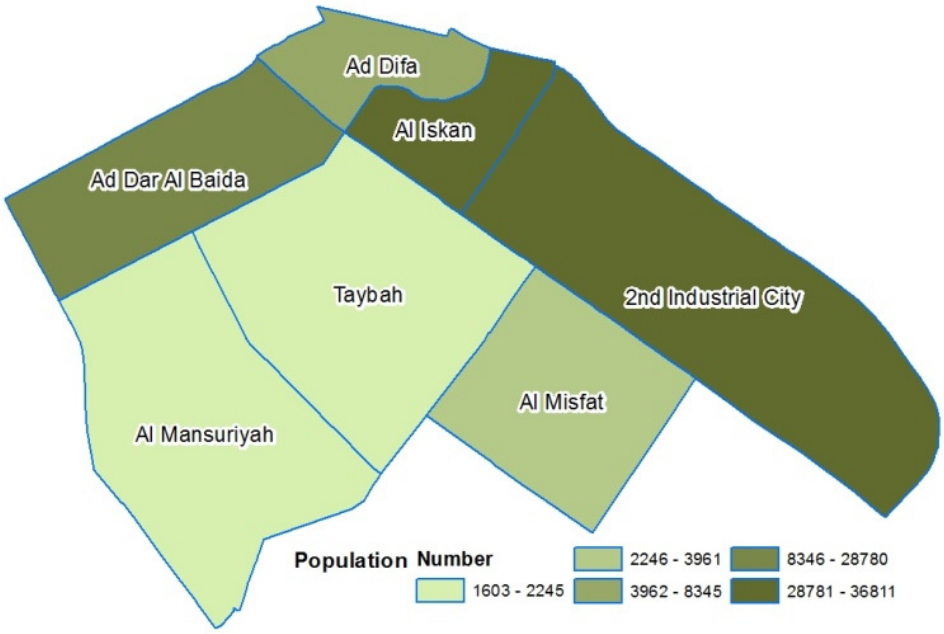

Figure 2. Population of the study area.

In the study area, two major industrial factories were established, namely the Second Industrial City and Al-Misfat (the Saudi Aramco Oil Refinery) (Figure 3). The Second

Industrial City was established in 1979 and has more than 823 factories with different activities [15]. The Al-Misfat refinery was established in 1974 and produces various kinds of petroleum derivatives. Moreover, there is heavy vehicular traffic throughout the day to support the industrial area.

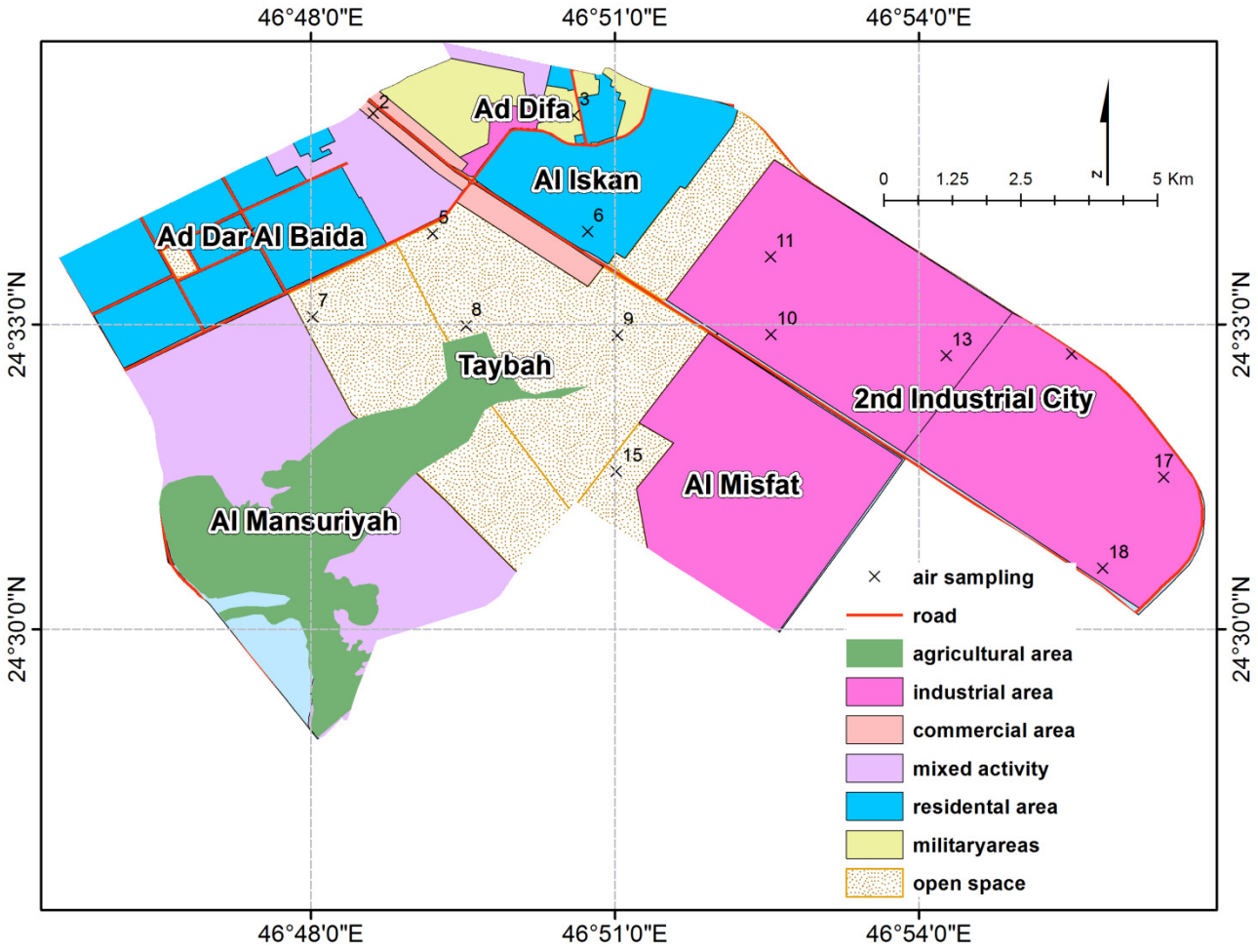

Figure 3. Land-use map of the study area and location of air sampling.

The western part of the study area is bounded by Wadi Hanifa, where the treated wastewater from Riyadh City is disposed. This water flows along the valley, with some agricultural activities in the Mansuriah and Taybah districts, which are less densely populated.

2.2. The Questionnaire

The study involved a survey about people's opinions regarding air pollution. The survey was conducted through a questionnaire, which was prepared in accordance with relevant guidelines and regulations and was approved by the Geography Department at King Saud University. Random samples of the population were chosen from the seven suburbs, and the questionnaire was distributed to 405 persons. The sub-samples, determined by the study, were according to population, as shown in Table S1.

The questionnaire consists of three parts: inhabitants' conditions, recognizing pollution, and pollution impact on the environment and health. The study applied chi-square and Cramer's V tests to understand the relationship between districts and pollution aspects.

2.3. Spatial and Temporal Analysis

Thermal analysis was carried out using the Landsat 8 satellite sensor image, and the land surface temperature (LST) was calculated from band 10 and band 11 by using land

surface emissivity (ε). In addition, the normalized difference vegetation index (NDVI) was calculated using band 4 and band 5 to determine the proportion of vegetation (*PV* and ε) to estimate the LST [32–35], as shown in Figure 4. Three images from May 2014, 2017, and 2020, with a ground resolution of 30 m, were selected.

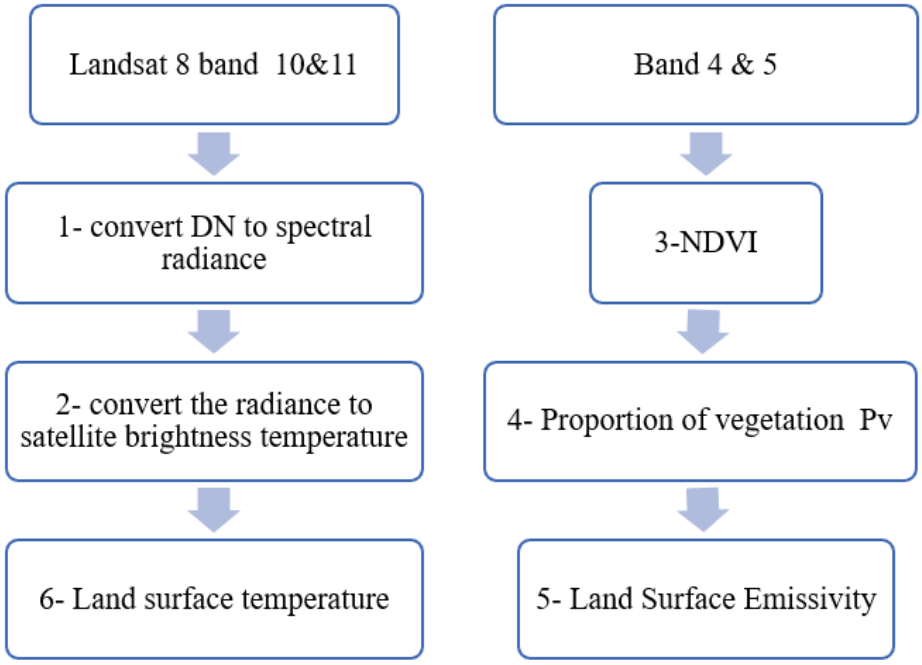

Figure 4. Flowchart to determine land surface temperature.

At the same time, the study involved the measurement of particulate matter (PM10, PM4, PM2.5, and PM1) and gases (CO, CO_2, NO, NO_2, SO_2, O_3, H_2S, and Volatile organic compounds VOCs) using portable instruments at 18 points from 18 to 25 May 2014. The measuring was according to Presidency of Meteorology and Environment Protection standards (PME) in Riyadh and performed by Geotechnical and Environmental Company (GECO), as shown in Table S2. The distance between sample sites was 2–3 km, as shown in Figure 3.

The study used descriptive analysis for air sampling, to picture and summarize the data [36], and used correlation coefficients to assess the strength of linear relationship between variables. Principal component analysis (PCA) was carried out to transform the original set of variables into a smaller set of linear combinations [37].

Data analysis was carried out geostatistically, using ArcGIS 10.1, while ordinary kriging was done by creating a semivariogram. The study estimated the central tendency, dispersion, and shape to determine the type of distribution of numerical variables. A semivariogram was created by building the spatial variability structure of each attribute, as in shown in Equation (1).

$$\gamma(h) = \frac{1}{2N(h)} \sum_{i=1}^{N(h)} [(Z(x) - Z(x+h)]^2 \quad (1)$$

where $\gamma(h)$ is the semi-variance, $Z(x)$ is the value of initial potential at site x, $Z(x + h)$ is the value of potential at site (h) distance apart from (x), and N is the number of sample pairs [38].

Ordinary kriging maps were established to predict values at a non-sampled point that assumes a constant unknown meaning, Equations (2a) and (2b):

$$Z(X_0) = \mu + \varepsilon(X_0) \quad (2a)$$

$$Z(X_0) = \sum \lambda_i \gamma(x_i), \quad \sum \lambda_i = 1 \tag{2b}$$

where μ is an unknown constant, $\varepsilon(X_0)$ is the the error associated with an unknown location X_0, $Z(X_0)$ is the estimated value of Z at X_0, and λ_i is the the weight that gives the best-possible estimation from the surrounding points.

Finally, the trend of the monthly average of NO_2 and PM10 concentrations was determined for the Southern Ring Road air station from January 2016 to September 2018 and the Al-Khaldiyah air station from September 2019 to May 2020. These two air stations were selected as they are the closest to the study area and have air quality conditions similar to those in the study area. Moreover, a continuous data set for the time period mentioned above was available from these two air-quality-monitoring stations.

3. Results

3.1. The Questionnaire

Most respondents (nearly 64.85%) were in the age group of 20–40 years. Of these, 85.11% are employees (private sector or government), and their housing is near their workplace. Half of them are professionals and are living in the study area for more than 10 years.

Most of the respondents reported that the buildings they live in are dirty, the plants are dusty, and fine dusty clouds extending about 1–3 km or more are present around the residential buildings, as shown in Figure 5.

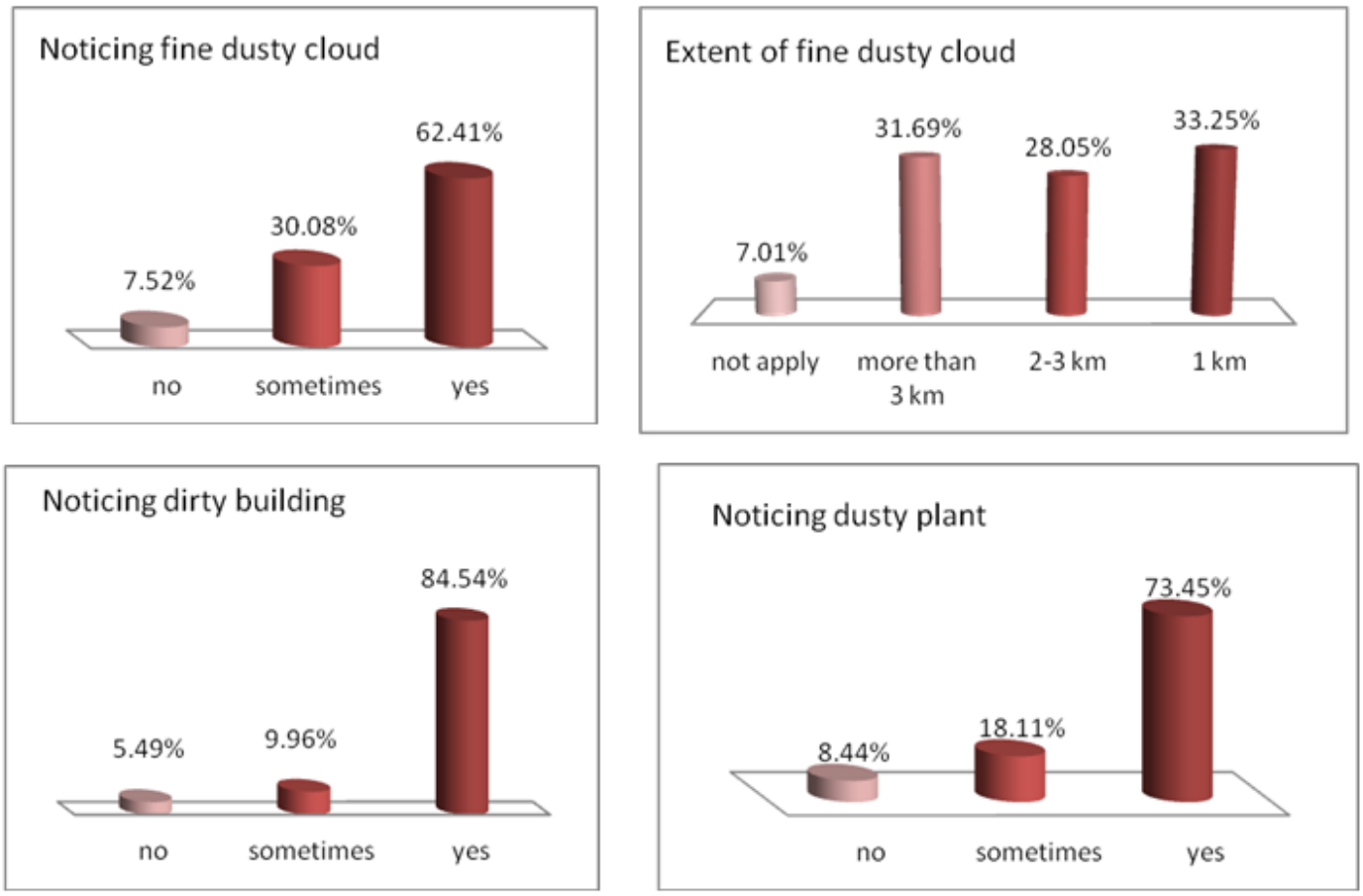

Figure 5. Noticing the pollution aspects in the study area.

They reported that most of the aspects related to air quality are similar in many residential districts of Riyadh; however, the problem of dirty buildings is specific to the study area, as shown in Table S3. Al-Iskan, Ad-Dar Al-Baida, and the Second Industrial

City are the most heavily polluted districts in the study area; and as a consequence, their residents suffer from many respiratory and eye diseases, as shown in Figure 6.

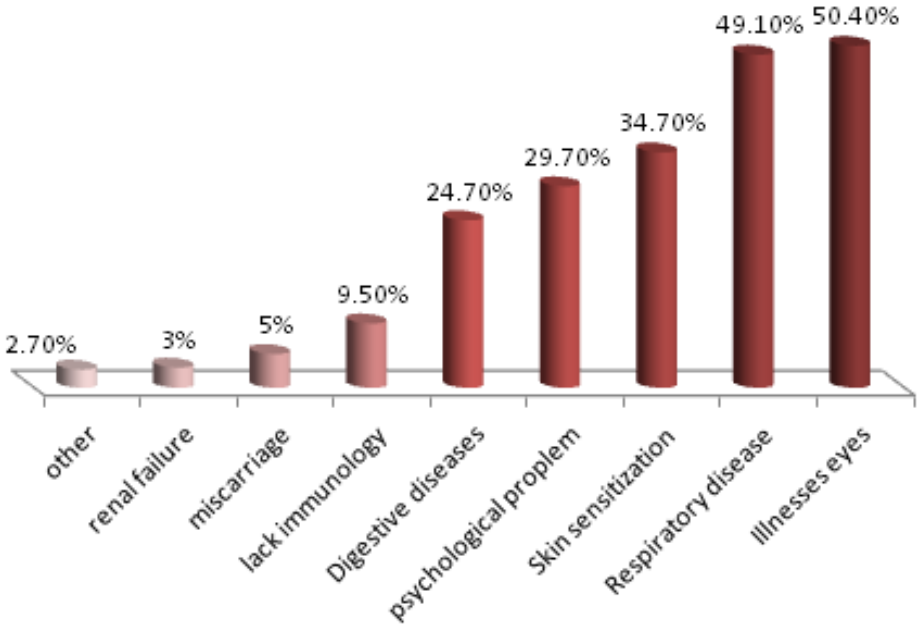

Figure 6. Diseases the population suffers from due to air pollution.

The survey results confirm the existence of problems related to air pollution in the study area. Field measurements and spatial analysis of gases and particulate matters, suspended in the air, are required to determine the extent and concentration of pollutants.

3.2. Thermal Analysis

The study widely used the NDVI as an indicator of the vegetation index and to calculate the LST. Generally, the study area shows a high variation in temperature. The highest temperature is observed in Al-Misfat, the factories, and the Second Industry City. The NDVI imageries from 2014 to 2020 (Figure 7) showed low values in most of the study area, except in the agricultural area in Taybah and Al-Mansuriah. The NDVI showed a gradual decrease in the study area, showing a steady increase in temperature. However, in May 2020, a lower temperature was recorded as much of the activities had stopped due to the lockdown to prevent the spread of COVID-19. This observation proves that human activities and reduced vegetation cover are major reasons for the development of heat islands in the region.

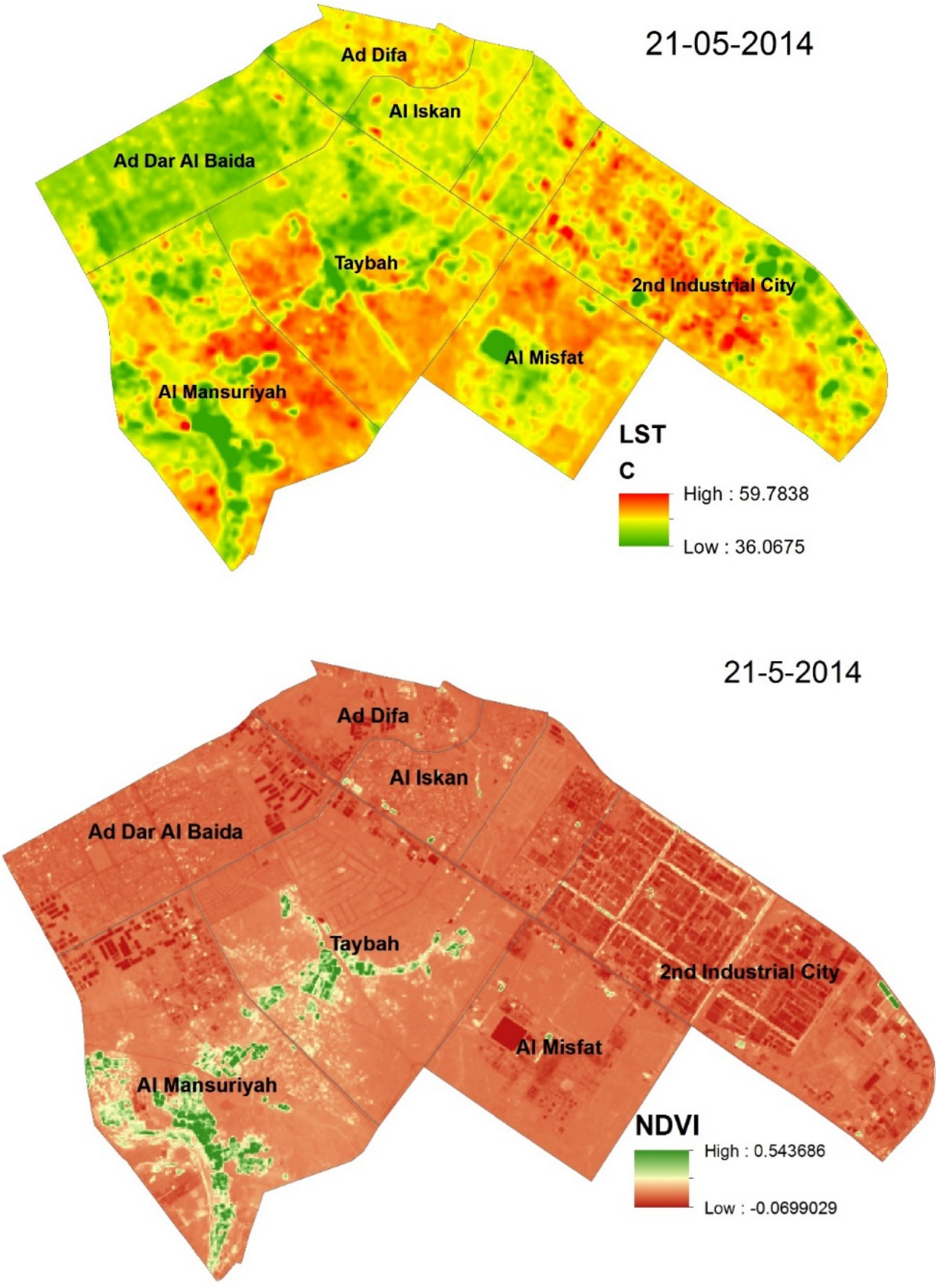

Figure 7. *Cont*.

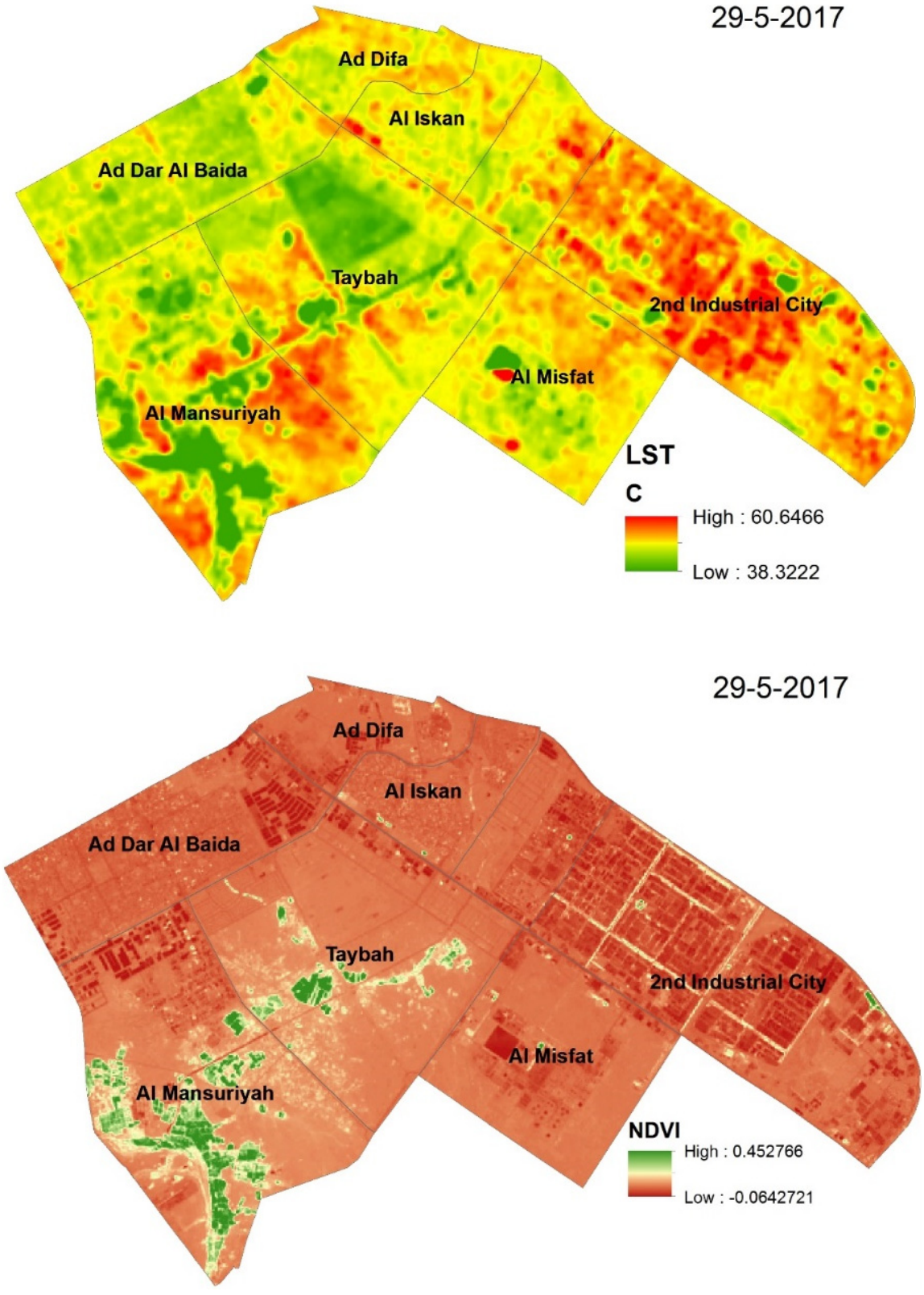

Figure 7. *Cont.*

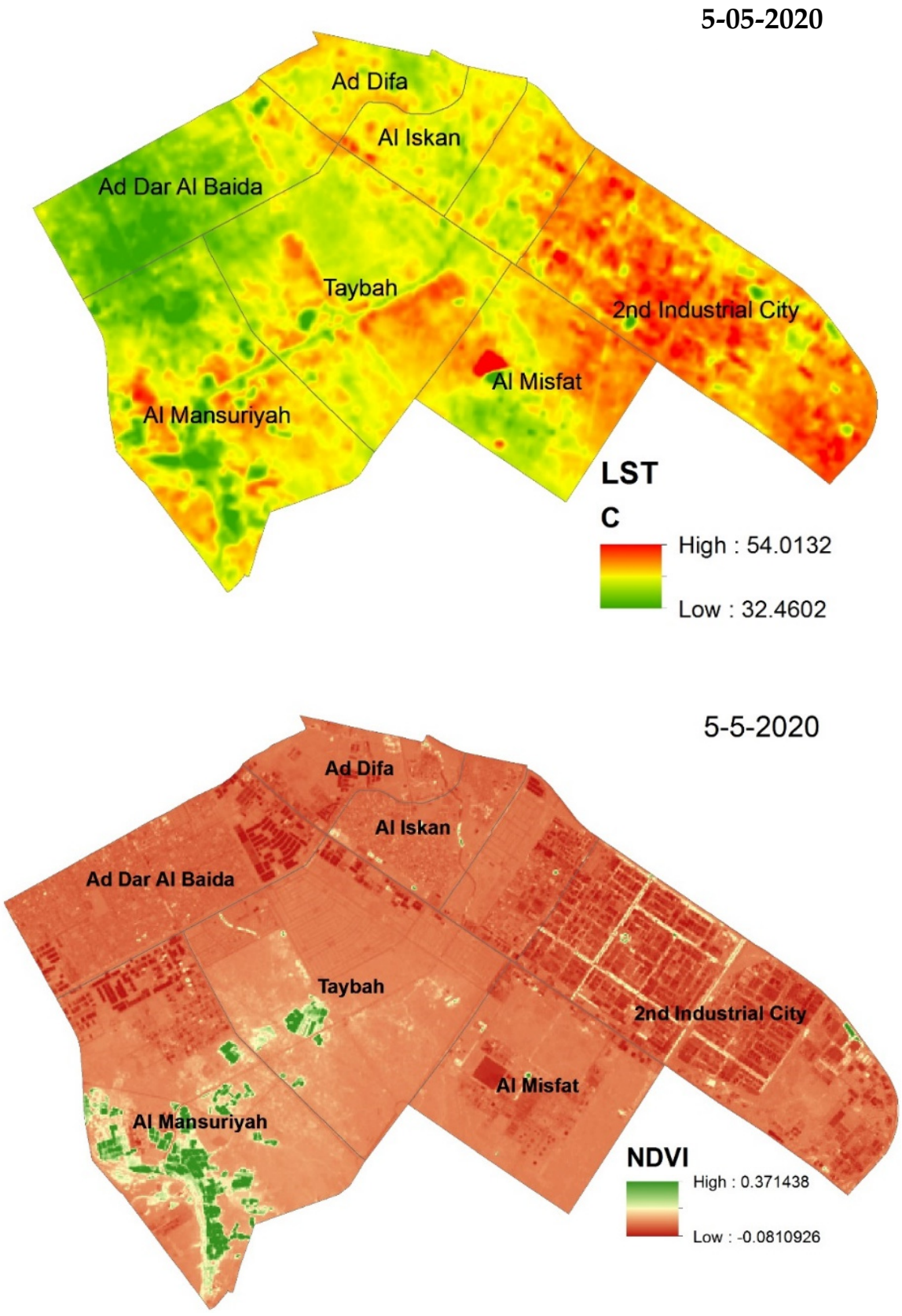

Figure 7. Land surface temperature and the normalized difference vegetation index (NDVI) (2014–2020).

3.3. Statistical and Geostatistical Analysis

The results of the descriptive statistics are given in (Table 1). The mean values of the particulate matter observed in the study area during most days of the year exceed the National Ambient Air Quality Standards (NAAQS).

Table 1. Descriptive statistics of air parameters.

	PM10 ug/m^3	PM2.5 ug/m^3	CO ppm	PM4 ug/m^3	PM1 ug/m^3	NO_2 ug/m^3	SO_2 ug/m^3	O_3 ppm	H_2S ug/m^3	VOC ug/m^3	CO_2 ug/m^3	NO ug/m^3
Mean	214	119	5	133.6	58.4	35	288	0.014	0.25	0.07	23.3	1.5
Minimum	78	28	2	38	11	9	110	0.01	0.07	0	4.7	0.2
Maximum	307	187	10	245	136	64	510	0.02	0.95	0.23	65	3.9
Std. deviation	79	58	2.8	62.5	44.2	15.5	108	0.005	0.23	0.06	15.7	0.99
Skewness	−0.22	−0.28	0.36	0.2	0.52	0.54	0.45	0.24	1.9	1.1	1.4	0.99
Kurtosis	−0.7	−0.7	−0.3	−0.2	−0.1	−0.55	0.05	−0.2	0.7	1	1.9	0.74
NAAQS	150	35	35			100	1300	0.075				

PM, particulate matter; NAAQS, National Ambient Air Quality Standards.

The correlation coefficient shown in Table S4 shows strong-to-moderate correlation between particulates, CO_2, CO, and NO_2 and indicates the same source of pollution.

Factor analysis (PC) helped in identifying four factors having eigen values of >1. The four factors explain 82.046% of the total variance, as shown in Table S5. PC1 accounts for 41.2% of the data variability and shows significant factor loadings of PM1, PM2.5, PM4, PM10, CO, and NO_2, as shown in Table S6. These variables have strong-to-moderate correlation, as shown in Table S4. PC2 represents 14.5% of the total variability and has significant factor loadings of SO_2 and CO_2. PC3 and PC4 represent 13.6% for O_3 and VOCs and 12.756% for H_2S and NO, respectively.

Ordinary kringing maps were built, as shown in Figure 8, for the particulate matter and gases, except O_3 because there was no significant spatial variation, as seen in the semivargrom model shown in Table S7. The distribution of all variables was lognormal for different types of the chosen model, depending on the least mean square error.

High concentrations of pollutants and particulate matter are in Al-Misfat, the Second Industrial City, and along the highway.

The concentration of PM varies in the study area, depending on land use and working conditions. However, a high concentration of coarse particulate matter (PM10) covers large areas, and its mean (214 ug/m^3) exceeds the standard limit (150 ug/m^3). Fine particulates (smaller than 2.5) are more critical and may cause more respiratory problems. They are concentrated in specific areas around Al-Misfat and the Second Industrial City. These fine particulates, derived mostly from combustion, may remain suspended for weeks and drift for many kilometers [39]. Moreover, spatial distributions of particulates are similar to those of CO and NO_2 and consequently considered to be within PC1.

A high variation in the concentration of oxides, CO_2, NO_2, and SO_2, is observed in the study area. The highest concentrations are around the Second Industrial City and Al-Misfat, where industries and automobile emissions are considered as the major sources of NO_2 [20]; however, emissions remained below standard at all places. VOC emission is concentrated in Al-Misfat and in the southeastern part of the Second Industrial City. The oil and natural gases sector is the main source of VOCs. H_2S is concentrated in the urban area in the northern part of the study area and near Al-Misfat. The main sources of H_2S are petroleum refineries, Al-Misfat, and the sewage system. Ad-Dar Al-Baida suffers from the leakage of an old sewage system, and the population suffers greatly from stagnant sewage pools and bad smells.

PM10 and NO_2 concentrations showed a continuous increase from 2016 to 2019. However, they clearly decreased during the spring of 2020 by 62% and 78%, respectively, due to the lockdown imposed during the coronavirus pandemic, as shown in Figure 9, wherever human activity decreased dramatically.

The southern part of the study area suffers from pollution, mainly particulate matter from factories and dust storms. In addition, vehicles are one of the main causes of air pollution and emissions of carbon from PM2.5 [21]. Ad-Dar Al-Baida, Taybah, and Al-Mansuriah are the least affected due to their distance from the industrial area. Despite that, Ad-Dar Al-Baida residents complain of pollution, and remeidial measures must be adopted to reduce the seriousness of the situation. More studies should be conducted in the study area to determine the general direction of the concentrations of oxides and to identify the chemical composition of the particulate matter.

Moreover, citizens may change their lifestyle to mitigate the sources of air pollution, such as transportation and energy consumption [40].

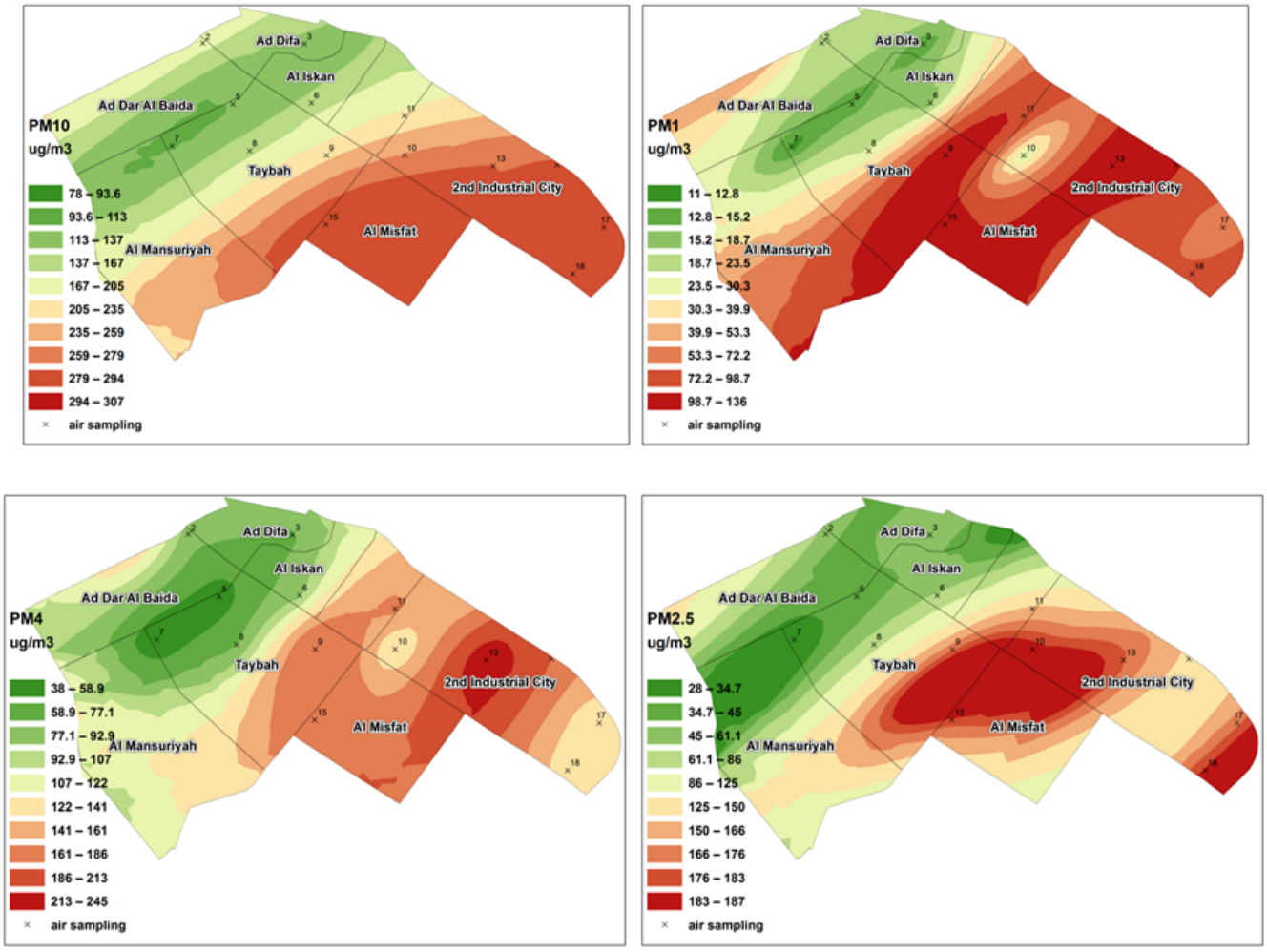

Figure 8. *Cont.*

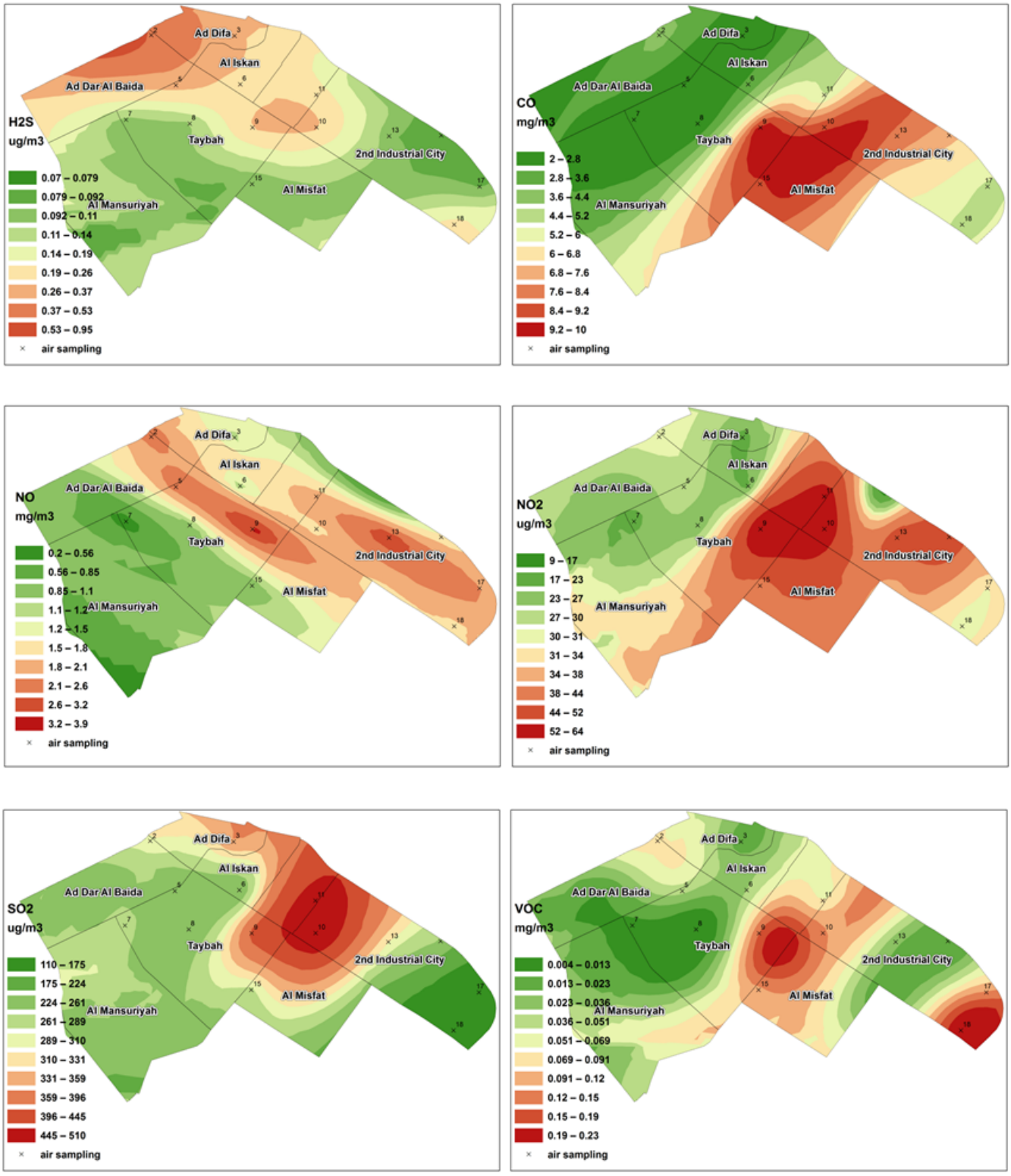

Figure 8. Ordinary kriging map of particulate matter and gases.

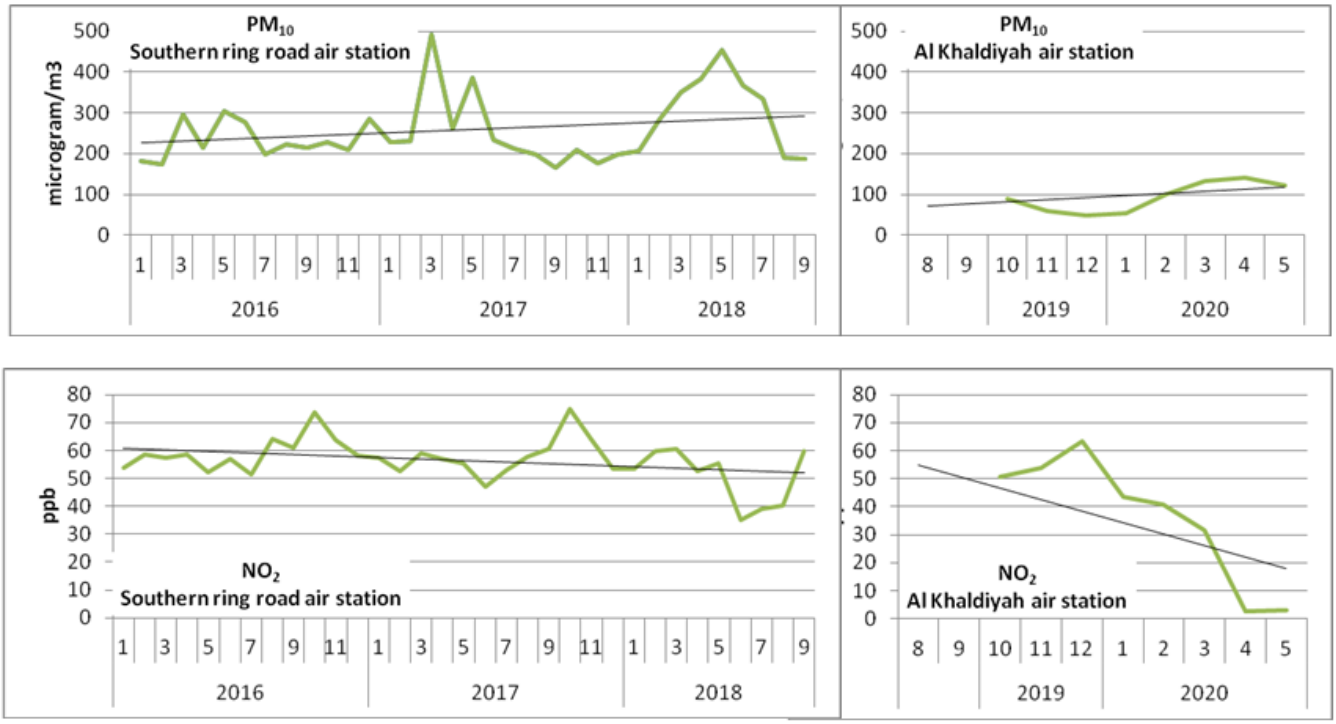

Figure 9. Trend in PM10 and NO_2 during 2016–2020 on the Southern Ring Road and the Al Khaldiyah air station.

4. Conclusions

This study based on the questionnaire responses of residents living in southern Riyadh and air quality monitoring from 2016 to 2020 from a couple of air-monitoring stations close to the area of interest reveals that the adverse effects of poor air quality due to urbanization and industrialization are mostly felt by the residents of Al-Iskan, Ad-Dar Al-Baida, and the Second Industrial City. Respiratory problems and irritation in the eyes were reported by 49% and 50% of the residents, respectively, during the survey. A high concentration of PM10 has been observed in many places in the study area, and it exceeds the permissible limits. Thermal analysis of the area showed the maximum temperature in the Second Industrial City and Al-Misfat, indicating the presence of the thermal island effect in these regions due to industrial activities. The anthropogenic influence on air quality was evident from the air quality data for 2020, which showed a marked decrease in parameters such as NO_2 due to the impacts of lockdown on various activities during the coronavirus pandemic. The land surface temperature image for May 2020 showed a temperature range between 54 °C and 32.4 °C, which is less than the temperature recorded during the same period in 2014 and 2017 and clearly shows the positive impact of minimal commercial/industrial activity during the lockdown period in 2020.

Supplementary Materials: The following are available online at https://www.mdpi.com/2076-3417/11/5/2107/s1, Table S1: Distribution of questionnaire in the study area; Table S2: Air sampling methods and instruments; Table S3: Relationship between districts and impact of pollution; Table S4: Correlation coefficients at 95% confidence level; Table S5: Eigen values of PC of the data sets; Table S6: Principal Component loadings of the data sets; Table S7: Semivariogram parameters.

Author Contributions: A.S. wrote the main manuscript and interpreted the data; M.A.-T. prepared questioners and analyzed the statistical data; S.H.-E. analyzed the Landsat images; F.K.Z. drafted and editing the work; N.A.-D. designed maps and prepared Figures 1–3. All authors have read and agreed to the published version of the manuscript.

Funding: This research was funded by the Deanship of Scientific Research at King Saud University through research group number RG-1438-023.

Institutional Review Board Statement: Not applicable.

Informed Consent Statement: Not applicable.

Data Availability Statement: Data sharing not applicable.

Acknowledgments: Sincere thanks to the Royal Commission for Riyadh City and the General Authority of Meteorology and Environment Protection for providing air quality data.

Conflicts of Interest: The authors declare no conflict of interest.

References

1. Al-Jelani, H. Air quality assessment at Al-Tan'eem area in the Holy Makkah City, Saudi Arabia. *Environ. Monit. Assess.* **2009**, *156*, 211–222. [CrossRef]
2. Vicente, A.B.; Jordan, M.M.; Sanfeliu, T.; Sánchez, A.; Esteban, M.D. Air pollution prediction models of particles, As, Cd, Ni and Pb in a highly industrialized area in Castellón (NE, Spain). *Environ. Earth Sci.* **2012**, *66*, 879. [CrossRef]
3. Pekey, B.; Özaslan, Ü. Spatial distribution of SO_2, NO_2, and O_3 Concentrations in an Industrial City of Turkey using a passive sampling method. *Clean Soil Air Water* **2013**, *41*, 423–428. [CrossRef]
4. Al-Harbi, M. Assessment of Air Quality in two Different Urban Localities. *Int. J. Environ. Res.* **2014**, *8*, 15–26.
5. Farahat, A. Air pollution in the Arabian Peninsula (Saudi Arabia, the United Arab Emirates, Kuwait, Qatar, Bahrain, and Oman): Causes, effects, and aerosol categorization. *Arab. J. Geosci.* **2016**, *9*, 1–17. [CrossRef]
6. WHO. *Air Quality Guidelines: World Health Organization, Global Update WHO Regional Office for Europe 2006*; WHO: Copenhagen, Denmark, 2005.
7. GHODR. *Urban Outdoor Air Pollution, Burden of Disease by Country, Global Health Observatory Data Repository*; World Health Organization: Geneva, Switzerland, 2008. Available online: http://apps.who.int/gho/data/node.main.285 (accessed on 10 February 2021).
8. IARC. *Outdoor Air Pollution as a Leading Environmental Cause of Cancer Deaths*; International Agency for Research on Cancer, World Health Organization: Lyon, France, 2013. Available online: http://www.iarc.fr/en/media-centre/pr/2013/pdfs/pr221_E.pdf (accessed on 10 February 2021).
9. Bourdrel, T.; Bind, M.A.; Béjot, Y.; Morel, O.; Argacha, J.F. Cardiovascular effects of air pollution. *Arch. Cardiovasc. Dis.* **2017**, *110*, 634–642. [CrossRef]
10. Canadian Medical Association. No Breathing Room: National Illness Costs of Air Pollution. 2008. Available online: http://www.healthyenvironmentforkidsca/sites/healthyenvironmentforkids.ca/files/No_Breathing_Room.pdf (accessed on 10 February 2021).
11. Nyberg, F.; Gustavsson, P.; Järup, L.; Bellander, T.; Berglind, N.; Jakobsson, R.; Pershagen, G. Urban air pollution and lung cancer in Stockholm. *Epidemiology* **2000**, *11*, 487–495. [CrossRef]
12. Nafstad, P.; Haheim, L.L.; Oftedal, B.; Gram, F.; Holme, I.; Herrmann, I.; Leren, P. Lung cancer and air pollution: A 27 year follow up of 16 209 Norwegian men. *Thorax* **2003**, *58*, 1071–1076. [CrossRef]
13. Al-Ahmadi, K.; Al-Zahrani, A. NO_2 and Cancer Incidence in Saudi Arabia. *Int. J. Environ. Res. Public Health* **2013**, *10*, 5844–5862. [CrossRef]
14. ADA 2017, Regional Plan for the Region Riyadh, Al-Riyadh Development Authority. Available online: http://www.ada.gov.sa/ADA_A/DocumentShow/?url=/res/ADA/Ar/Projects/regional_plan/index.html (accessed on 10 February 2021).
15. Modon. Industrial Cities Directory, Saudi Industrial Property Authority. 11\12\2016 9.12pm; 2017. Available online: http://www.modon.gov.sa/EN/INDUSTRIALCITIES/INDUSTRIALCITIESDIRECTORY/INDUSTRIALCITIES/Pages/default.aspx (accessed on 10 February 2021).
16. Al-Jassir, M.; Shaker, A.; Khaliq, M. Deposition of Heavy Metals on Green Leafy Vegetables Sold on Roadsides of Riyadh City, Saudi Arabia. *Bull. Environ. Contam. Toxicol.* **2005**, *75*, 1020–1027. [CrossRef]
17. Parrish, D.; Kuster, W.C.; Min, S.; Yokouchi, Y.; Kondo, Y.; Goldan, P.; De Gouw, J.; Koike, M.; Shirai, T. Comparison of air pollutant emissions among mega-cities. *Atmos. Environ.* **2009**, *43*, 6435–6441. [CrossRef]
18. Al-Rehaili, A. Outdoor-indoor Air Quality in Riyadh: SO_2, NH_3, and HCHO. *Environ. Monit. Assess.* **2002**, *79*, 287. [CrossRef] [PubMed]
19. Tawabini, B.; Lawal, T.; Shaibani, A.; Farahat, A. Morphological and Chemical Properties of Particulate Matter in the Dammam Metropolitan Region: Dhahran, Khobar, and Dammam, Saudi Arabia. *Adv. Meteorol.* **2017**, *2017*, 8512146. [CrossRef]
20. Shareef, M.; Husain, T.; Alharbi, B. Analysis of Relationship between O_3, NO, and NO_2 in Riyadh, Saudi Arabia. *Asian J. Atmos. Environ.* **2018**, *12*, 17–29. [CrossRef]
21. Bian, Q.; Alharbi, B.; Shareef, M.; Husain, T.; Pasha, M.; Atwood, S.; Kreidenweis, S. Sources of PM2.5 carbonaceous aerosol in Riyadh, Saudi Arabia. *Atmos. Chem. Phys.* **2018**, *18*, 3969–3985. [CrossRef]
22. Air Quality Index. General Authority of Meteorology and Environment Protection. 2020. Available online: https://www.pme.gov.sa/Ar/Environment/AirQuality/Pages/AQ-Dashboard.aspx (accessed on 10 February 2021).
23. Isaaks, E.H.; Srivastava, R.M. *An Introduction to Applied Geostatistic*; Oxford University Press: New York, NY, USA, 1989.

24. Carlon, C.; Critto, A.; Marcomini, A.; Nathanail, P. Risk based characterization of contaminated industrial site using multivariate and geostatistical tools. *Environ. Pollut.* **2001**, *111*, 417–427. [CrossRef]
25. Moral, F.; lvarez, P.; Canito, J. Mapping and hazard assessment of atmospheric pollution in a medium sized urban area using the Rasch model and Geostatistic techniques. *Atmos. Environ.* **2006**, *40*, 1408–1418. [CrossRef]
26. Moradi Dashtpagerdi, M.; Sadatinejad, S.J.; Zare Bidaki, R.; Khorsandi, E. Evaluation of Air Pollution Trend Using GIS and RS Applications in South West of Iran. *J. Indian Soc. Remote Sens.* **2014**, *42*, 179. [CrossRef]
27. Roy, D.P.; Wulder, M.A.; Loveland, T.R.; Woodcock, C.E.; Allen, R.G.; Anderson, M.C.; Helder, D.; Irons, J.R.; Johnson, D.M.; Kennedy, R.; et al. Landsat-8: Science and product vision for terrestrial global change research. *Remote Sens. Environ.* **2014**, *145*, 154–172. [CrossRef]
28. Weng, Q.; Lu, D.; Schubring, J. Estimation of land surface temperature–vegetation abundance relationship for urban heat island studies. *Remote Sens. Environ.* **2004**, *89*, 467–483. [CrossRef]
29. Aniello, C.; Morgan, K.; Busbey, A.; Newland, L. Mapping micro-urban heat islands using LANDSAT TM and a GIS. *Comput. Geosci.* **1995**, *21*, 965–967, 969. [CrossRef]
30. Weng, Q.; Yang, S. Urban Air Pollution Patterns, Land Use, and Thermal Landscape: An Examination of the Linkage Using GIS. *Environ. Monit. Assess.* **2006**, *117*, 463. [CrossRef] [PubMed]
31. CDSI. Census of Population and Housing Report in Administrative Region. Central Department of Statistic and Information. Internal Report. 2004. Available online: http://www.cdsi.gov.sa/english/ (accessed on 10 February 2021).
32. USGS. Landsat 8 Data Users Handbook—Section 5/Conversion of DNs to Physical Units. 2018. Available online: https://landsat.usgs.gov/landsat-8-l8-data-users-handbook-section-5 (accessed on 10 February 2021).
33. Syariza, M.A.; Jaelania, L.M.; Subehie, L.; Pamungkasb, A.; Koenhardonoc, E.S.; Sulisetyonod, A. Retrieval of sea surface temperature over Poteran island water of Indonesia with Landsat 8 TIRS image: A preliminary algorithm. In Proceedings of the International Archives of the Photogrammetry, Remote Sensing and Spatial Information Sciences 2015, Joint International Geoinformation Conference 2015, Kuala Lumpur, Malaysia, 28–30 October 2015; Volume XL-2/W4.
34. Anandababu, D.; Purushothaman, B.M.; Suresh, B.S. Estimation of Land Surface Temperature using LANDSAT 8 Data. *Int. J. Adv. Res. Ideas Innov. Technol.* **2018**, *4*, 177–186.
35. Solangi, G.; Siyal, A.; Siyal, P. Spatiotemporal Dynamics of Land Surface Temperature and Its Impact on the Vegetation. *Civ. Eng. J.* **2019**, *5*, 1753–1763. [CrossRef]
36. Brase, C.H. *Understanding Basic Statistics*; Brooks/Cole: Seattle, WA, USA, 2010; Volume 5.
37. Isa, D.E. Proceedings of the World Congress on Engineering. In *The Robust Principal Component*; WCE: London, UK, 2009; Volume I, p. 1.
38. Deutsch, C.V. *Geostatistical Reservoir Modeling*; Oxford UP: Oxford, UK, 2002.
39. Seaton, A.; MacNee, W.; Donaldson, K.; Godden, D. Particulate air pollution and acute health effects. *Lancet* **1995**, *345*, 176–178. [CrossRef]
40. Sofia, D.; Gioiella, F.; Lotrecchiano, N.; Giuliano, A. Mitigation strategies for reducing air pollution. *Environ. Sci. Pollut. Res.* **2020**, *27*, 19226–19235. [CrossRef] [PubMed]